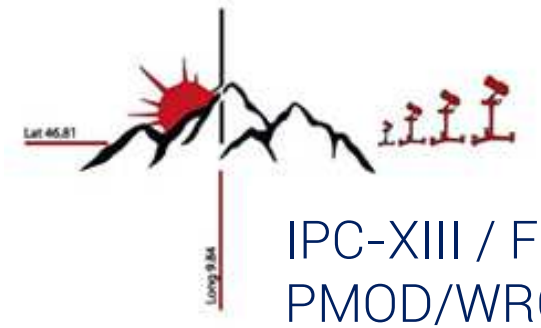

IPC-XIII / FRC-V / IPgC-III Symposium
PMOD/WRC (2021)

On the characterization of an AHF cavity radiometer and its traceability to WRR/SI

Presented by: José Balenzategui, CIEMAT (Spain)

Co-authored by: Balenzategui J.L., De Lucas J., González-Leiton A., Cuenca J., Molero M., Romero M.C., Fabero F., Silva J.P., Mejuto E., Sanz M., Escrivano D., Belenguer T., Ibañez F.

On the characterization of an AHF cavity radiometer and its traceability to WRR/SI

José Balenzategui
CIEMAT (Spain)

1. About us
2. Characterization of cavity radiometers
3. Basic aspects of AHF radiometer
4. Characterization results
5. Uncertainty budget
6. Traceability to WRR/SI
7. Conclusions

Ciemat
Centro de Investigaciones Energéticas, Medioambientales y Tecnológicas

1. About us

- → CIEMAT = Energy, Environment and Technology Research Center
- → Public research center, currently in the Ministry of Science and Innovation
- → Main headquarters located in Madrid (Spain), other local centers in Spain
- → Staff around 1250 people

1. About us

- → Photovoltaic Solar Energy Unit (Department of Energy).
- → Currently around 25 people, working since 1990 on research into polycristalline thin-film and deposited Si (a-Si:H, µ-Si) devices, and on testing of PV cells and modules, and arrays in PV solar plants.
- → **PVLab**: Laboratory for testing and calibration of solar irradiance sensors and photovoltaic devices.
- → Very large experience on outdoor calibration of pyranometers, pyrheliometers, solar cells, etc
- → Gaining Accreditation under ISO-IEC 17025 Standard for calibration of pyranometers (ISO9847), pyrheliometers (ISO9059) and shunts.

- → Collaboration with INTA (National Aerospacial Technology Institute) groups: Center for Metrology and Calibration (CMyC), and Space Optics Department. Framework of a research project (DEPRISACR, Spanish MSI R&D funds program)

2. Characterization of cavity radiometers

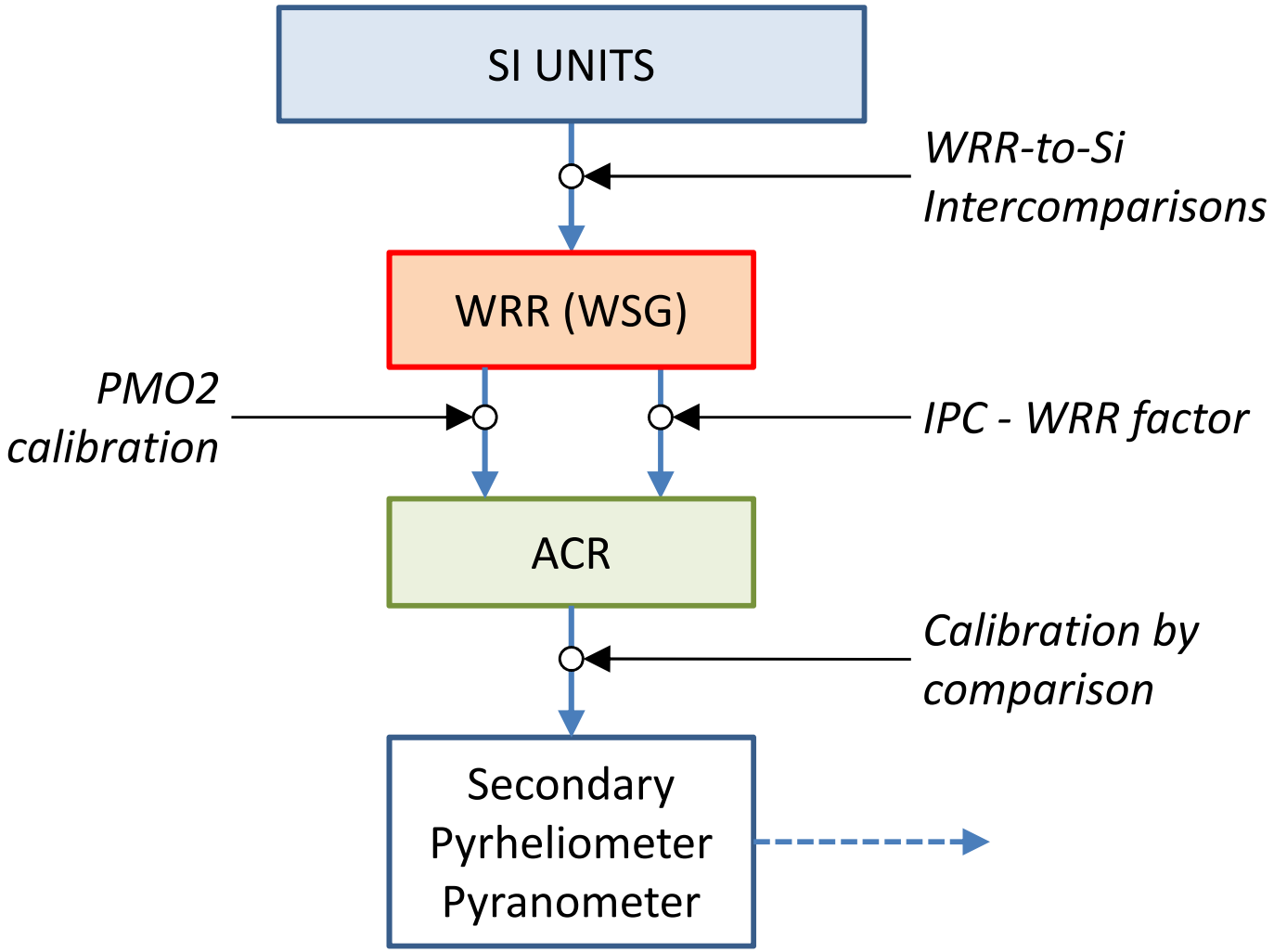

2. Characterization of cavity radiometers

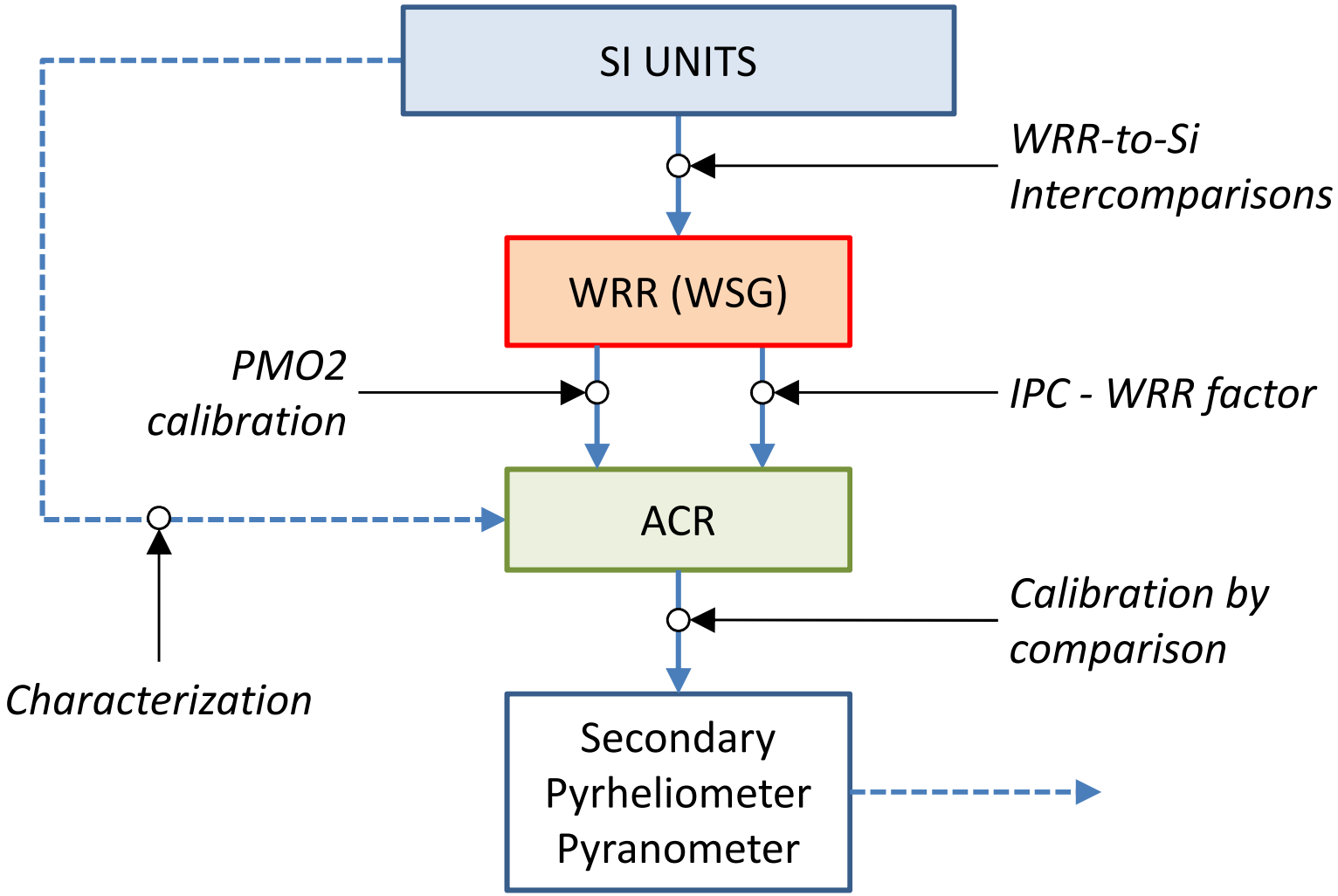

*"The purpose of **characterization** is to develop an understanding of the sources of error in the measurement process and how they affect specific measurement results"*

(NIST Engineering Statistics Handbook)

2. Characterization of cavity radiometers

This means *"identifying sources of error, quantifying errors and their effects on a specific reported value* [in our case, on solar irradiance] *in a statement of uncertainty"*
(NIST Engineering Statistics Handbook)

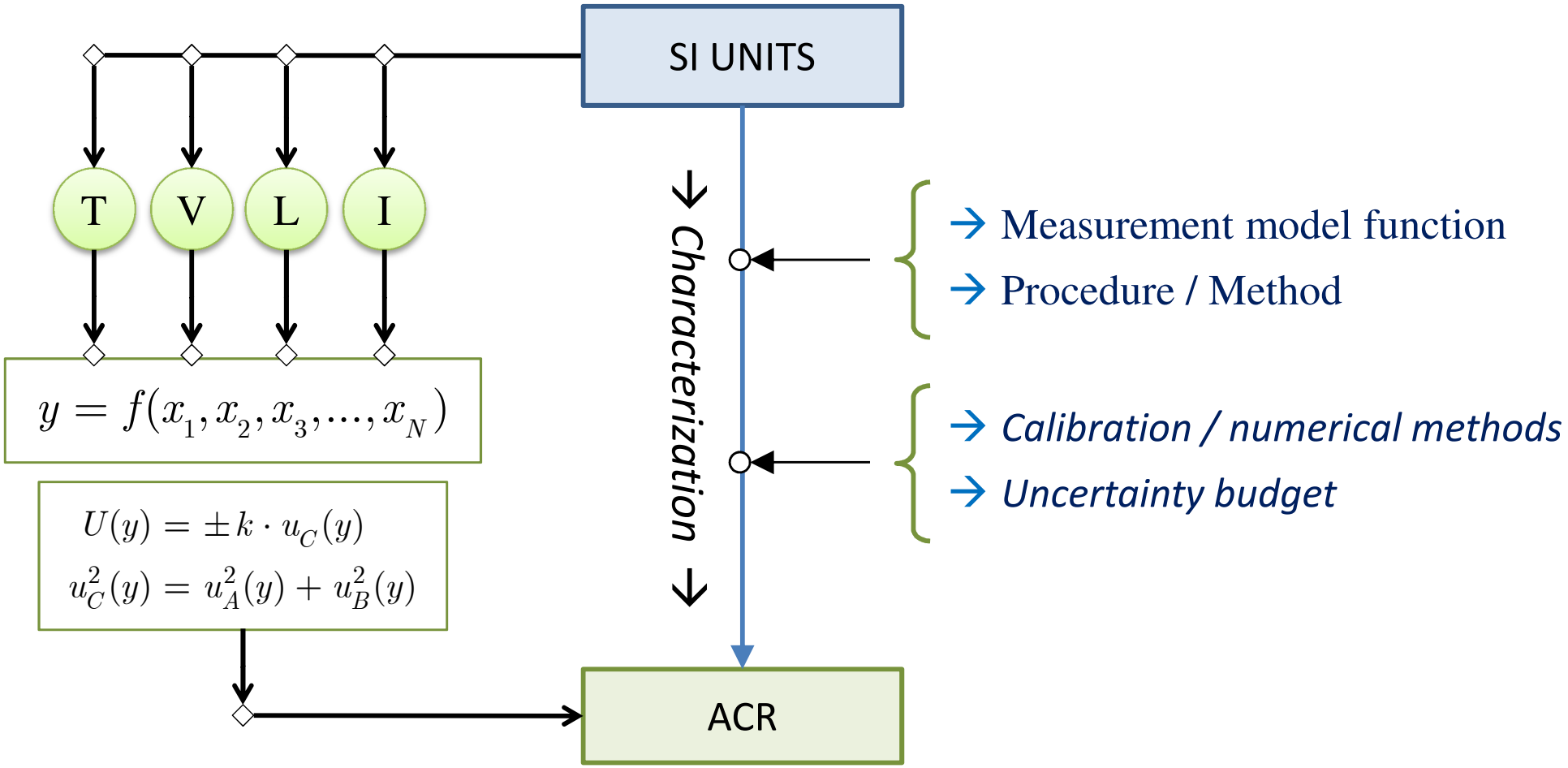

3. Fundamentals of AHF

- Passive-type cavity radiometer
- Double cavity structure on thermopile with a toroidal structure
- Precision aperture of 50 mm^2, FOV = 5°

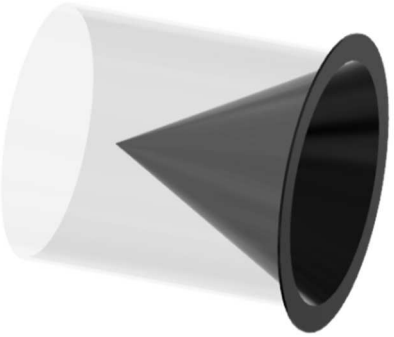

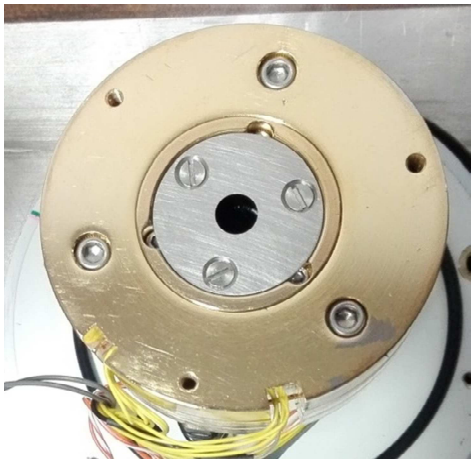

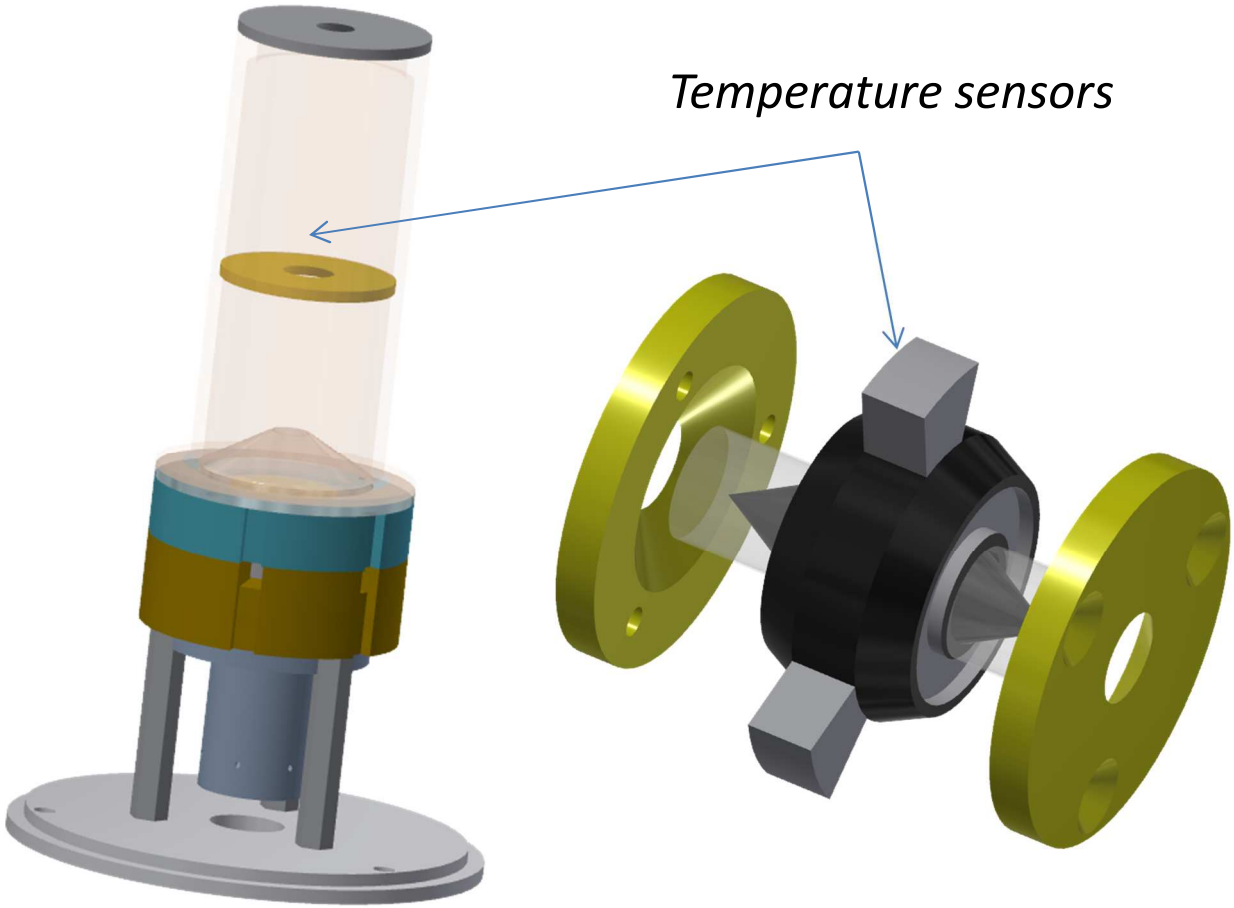

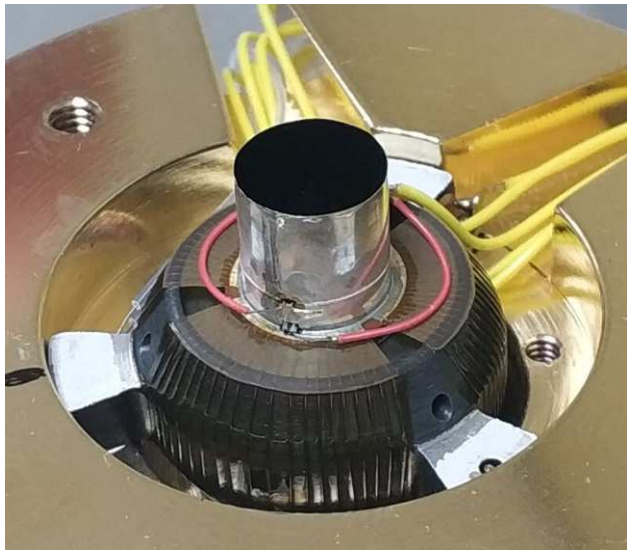

3. Fundamentals of AHF

➔ **Heater electrical circuit, sensing and operation mode**

– Head sensor + control box + external datalogger (DL)

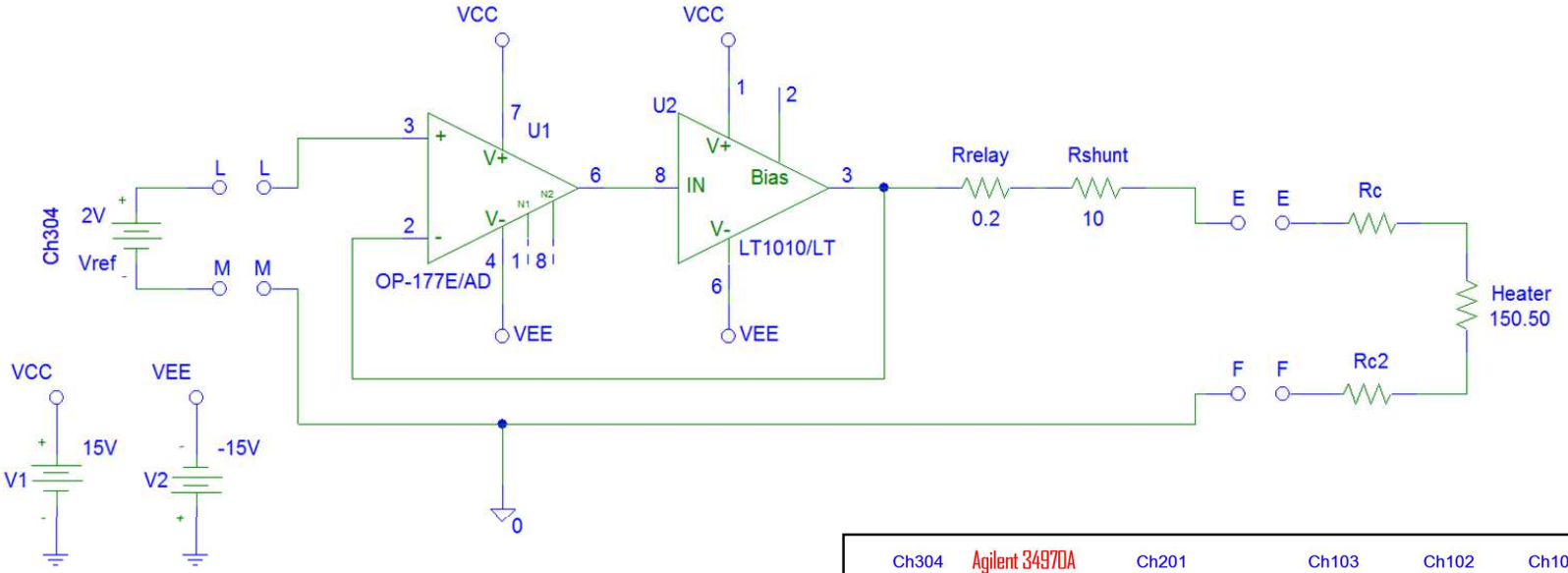

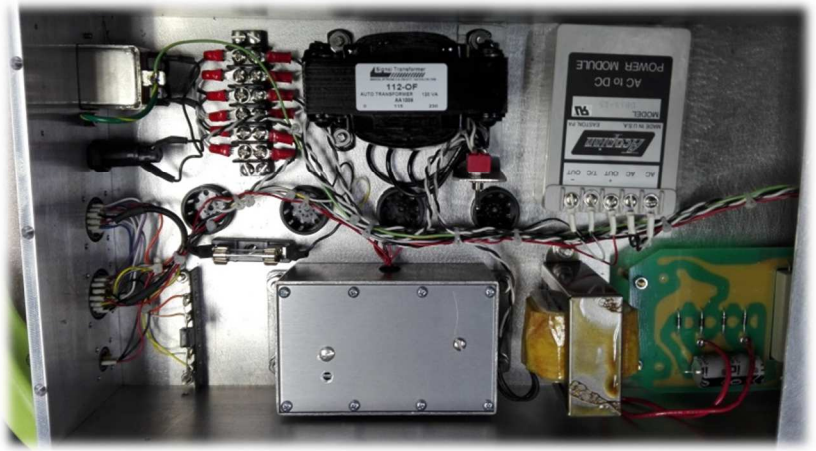

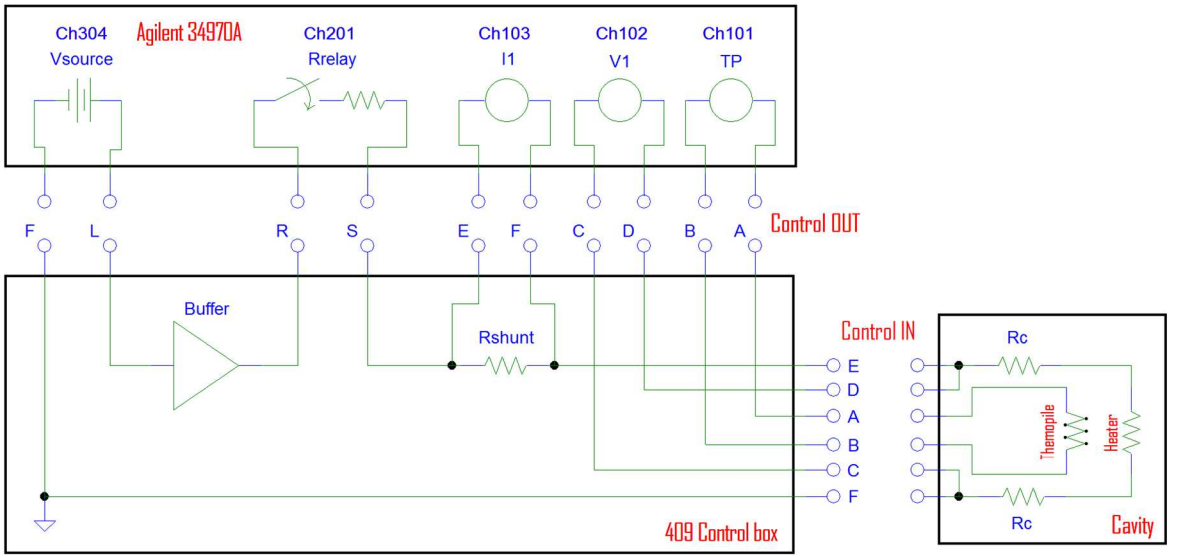

3. Fundamentals of AHF

→ (Radiant) solar power $P_S = A \cdot \alpha_C \cdot \gamma \cdot E \quad \rightarrow V_{TS} - V_{T0} = k_S \cdot P_S$

→ (Electrical) heater power $P_E = I_H \cdot V_H - I_H^2 \cdot R_C \quad \rightarrow V_{TE} - V_{T0} = k_E \cdot P_E$

→ Equivalence Principle: *if excitations powers are equivalent / indistinguishable to the effect of heating the cavity, the answer of the system will be the same*

$$P_E = P_S \quad \rightarrow V_{TS} - V_{T0} = V_{TE} - V_{T0} \quad \rightarrow k_E = k_S$$

→ Non-equivalence : *imperfections in the realization of this principle produce:*

$$k_E \neq k_S \quad \rightarrow \frac{k_E}{k_S} = L$$

→ Measurement model function:

$$E = \frac{L}{A \cdot \alpha_C \cdot \gamma}\left(\frac{V_{TS} - V_{T0}}{V_{TE} - V_{T0}}\right)\frac{V_I}{R_{SH}}\left(V_H - \frac{V_I}{R_{SH}}R_C\right)$$

$E = irradiance\ (W/m^2)$
$\alpha_C = cavity\ absorptance$
$\gamma = optical\ factor\ (collimator)$
$L = non - equivalence\ factor$
$V_{TX} = thermopile\ output\ (V)$
$I_H, V_H = heater\ current, voltage\ (A, V)$
$R_{SH} = shunt\ resistance\ (\Omega)$
$R_C = cavity\ cables\ resistance\ (\Omega)$

4. Characterization results

→ MMF:

$$E = \frac{L}{A \cdot \alpha_C \cdot \gamma}\left(\frac{V_{TS} - V_{T0}}{V_{TE} - V_{T0}}\right)\frac{V_I}{R_{SH}}\left(V_H - \frac{V_I}{R_{SH}}R_C\right)$$

Characterization

- Calibration of meter, aperture areas, resistances
- Estimation / simulation / numerical calculation of L, α_C, γ
- Testing / evaluation of non-explicit dependences (T, λ,…)
- Uncertainty budget

➔ **Calibration of the meter (DL)**

- Measurements & control based on an external Agilent 34970A DL
- Calibration carried out by the CMyC *Laboratory of Electricity* in INTA, with the highest accuracy and lower uncertainty attainables.
- Every channel calibrated according to its range of operation and magnitude

4. Characterization results

➔ Calibration of the precision aperture area

- Precision apertures of 8 mm diameter carefully drilled on disks made of Invar, 4 mm thick. Nominal area = 50 mm^2
- Carried out by the *Laboratory of Length and Precision Engineering* of the Centro Español de Metrología CEM (Spanish NMI)
- Vision machine (Mitutoyo Ultra Quick Vision 350 Pro) traced to SI, 360 points distributed along the aperture perimeter with resolution of 0.1 µm

A_{front} = 50.183 ± 0.0015 mm^2 (*k*=2)

A_{rear} = 50.163 ± 0.0015 mm^2 (*k*=2)

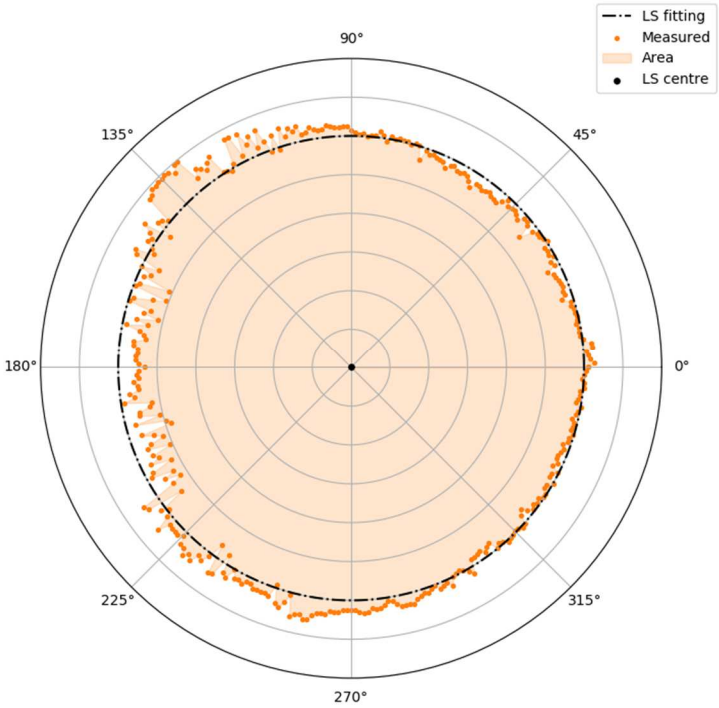

4. Characterization results

➔ Calibration of the resistance of the wires R_C

- Done by the TA *Calibration of Electrical Magnitudes* (PVLab-CIEMAT)
- Calibrated Keysight 34420A micro-ohmeter
- 4-wire connection with Accuprobe IK2C8C3D tips

$R_{C\text{-}D}$ = 25.1756 mΩ ± 0.0048 mΩ

$R_{A\text{-}B}$ = 25.8150 mΩ ± 0.0048 mΩ

R_T = 50.9907 mΩ ± 0.0067 mΩ (*k*=2)

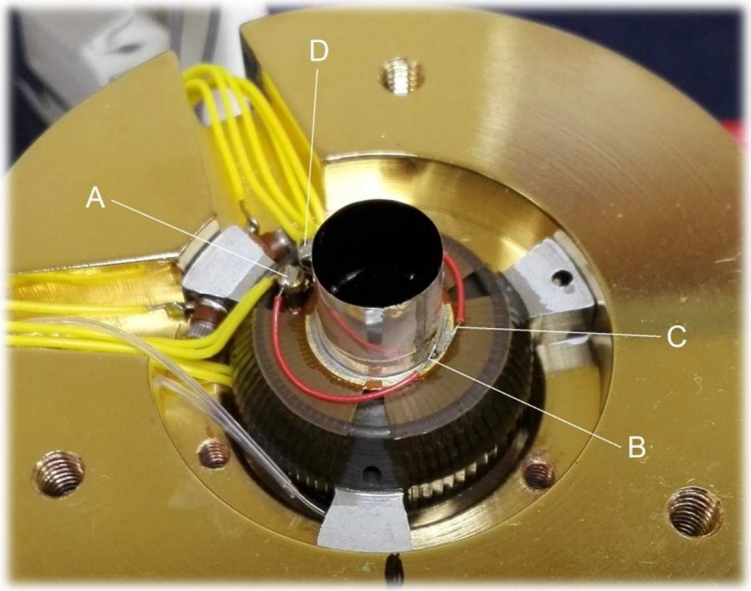

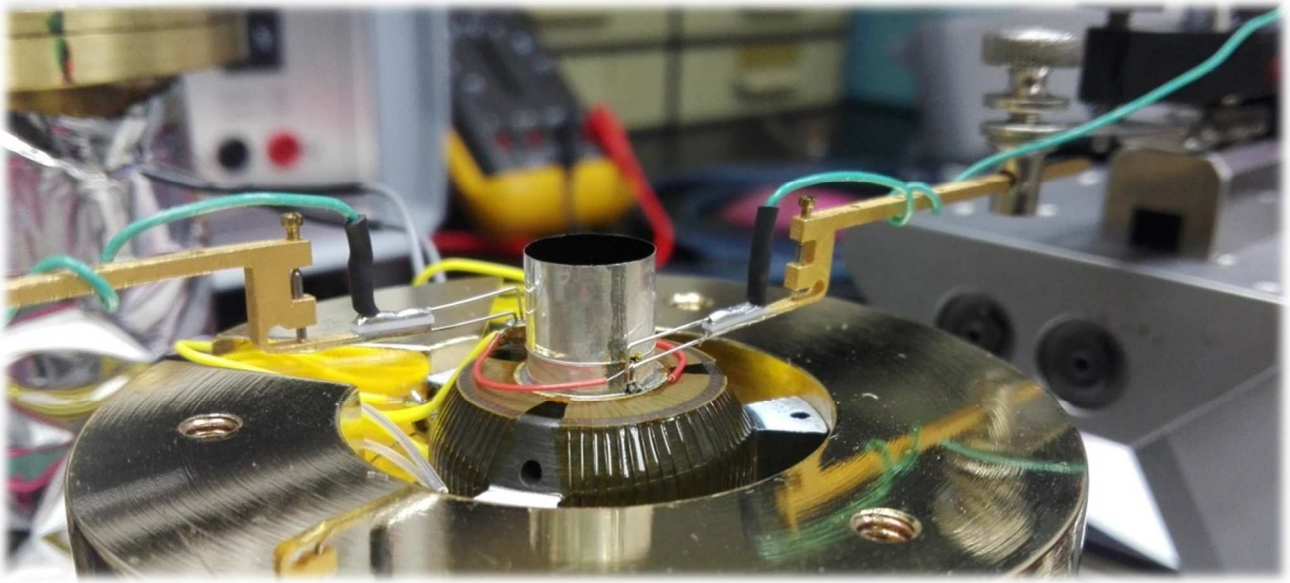

4. Characterization results

➔ Calibration of the shunt resistance R_{SH}

- Direct calibration carried out by the CMyC *Laboratory of Electricity* (INTA)
- Addition of a Pt100 sensor close to the shunt to control temperature drifts
- Test of temperature dependence of R_{SH} in the range 0º to 55ºC in a climatic chamber in the *Laboratory of Relative Humidity* (DI of CEM, Spanish NMI)

$$R_{SH} = 9.99869 \pm 0.00011\ \Omega \quad (k=2)$$

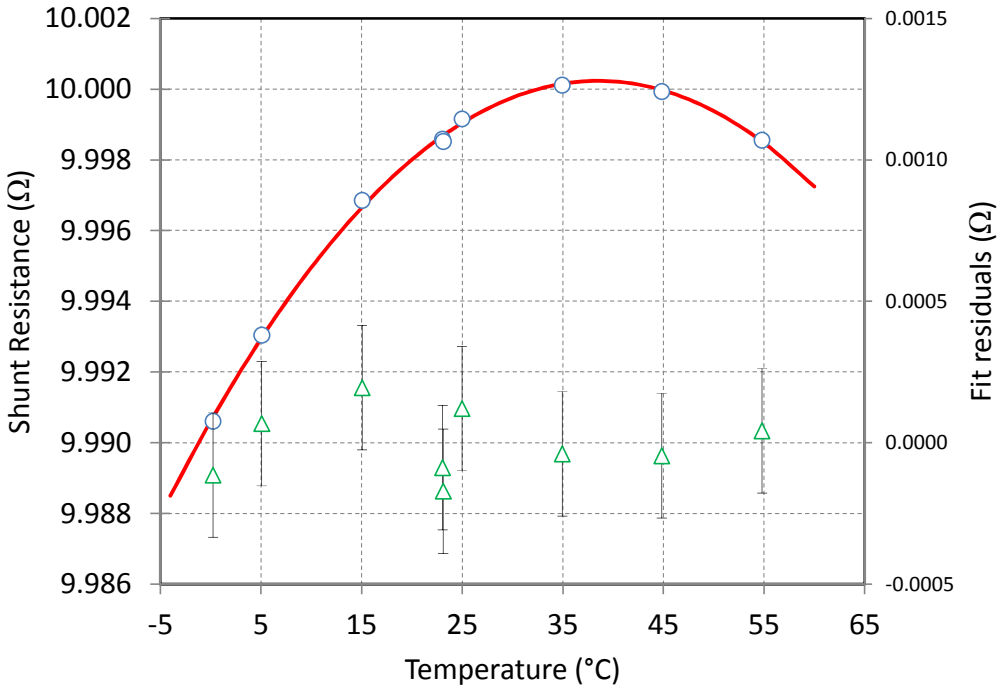

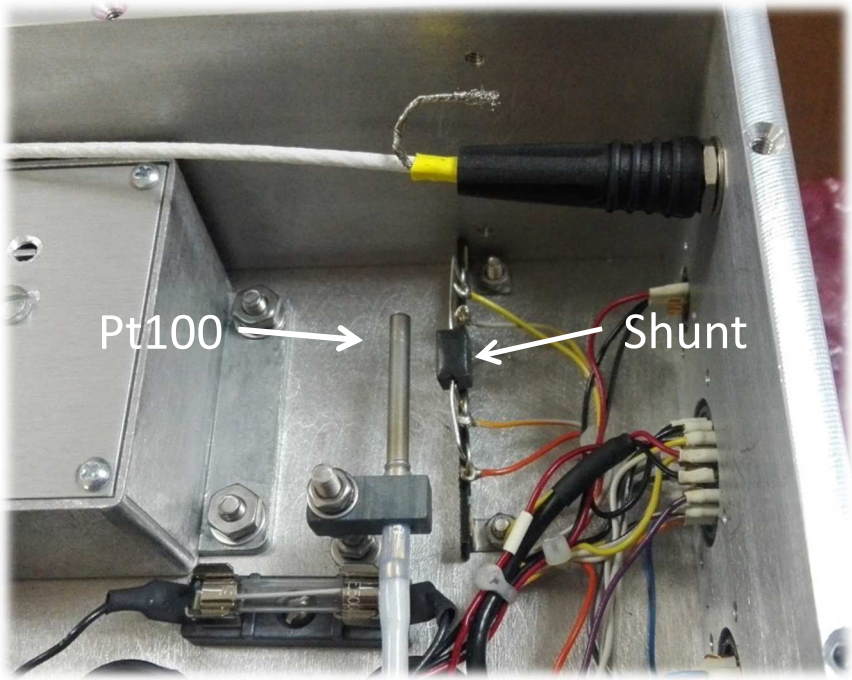

4. Characterization results

➔ Calibration of temperature sensors

- Calibration of YSI thermistors in the range 0º to 55ºC in a climatic chamber in the *Laboratory of Relative Humidity* (INTA)

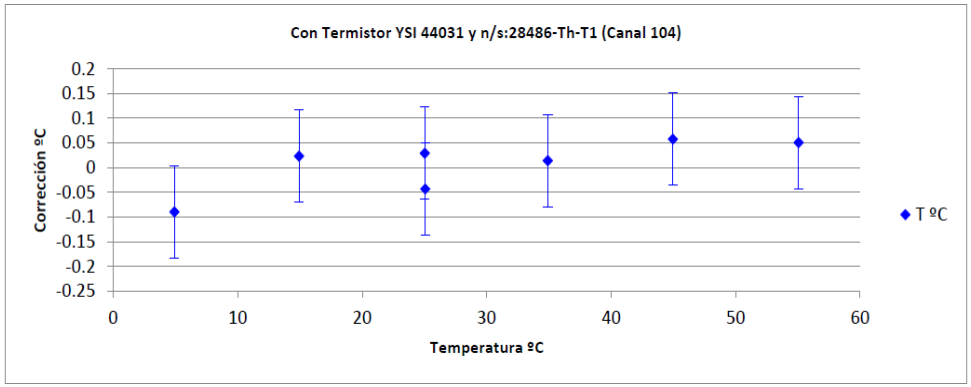

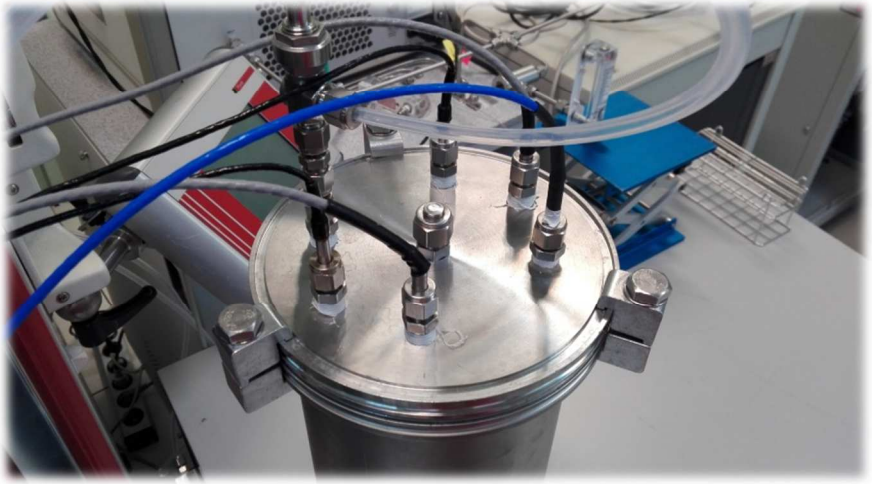

4. Characterization results

➔ Thermal characterization of *sensitivity*

– During calibration cycles, AHF software calculates a magnitude called *sensitivity* (mV/mW/cm^2), which is then used to calculate irradiance.

$$1/S = \frac{L}{A \cdot \alpha_C \cdot \gamma}\left(\frac{1}{V_{TE} - V_{T0}}\right)P_E \qquad E = \frac{V_{TS} - V_{T0}}{S}$$

– Temperature affects the evolution of the sensitivity (daily/inter-daily) and it seems to be also related to the "arms-up" effect in first runs.

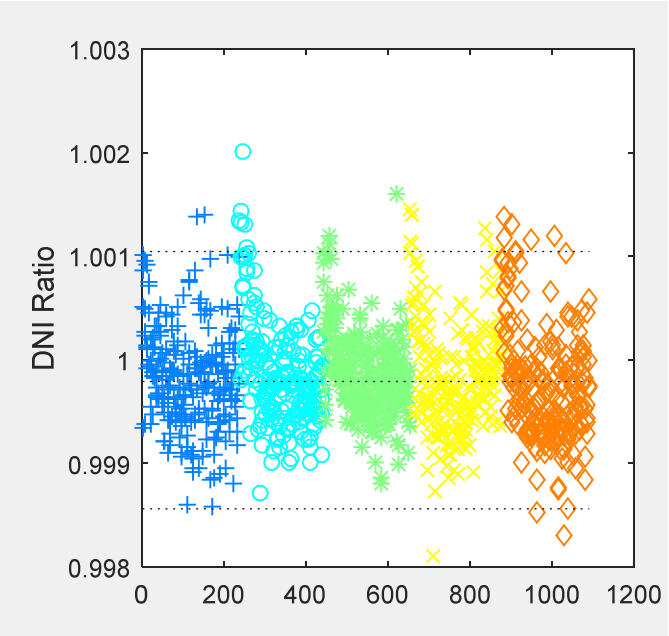

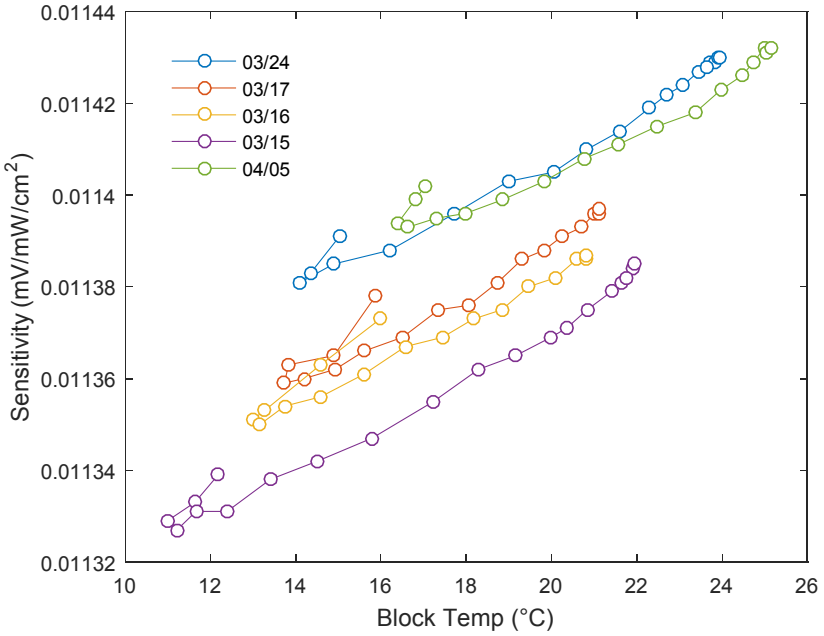

4. Characterization results

➔ Thermal characterization of sensitivity

- Specific experiment for testing dependence of sensitivity on T in a climatic chamber while AHF was illuminated with an external radiant souce (green laser)

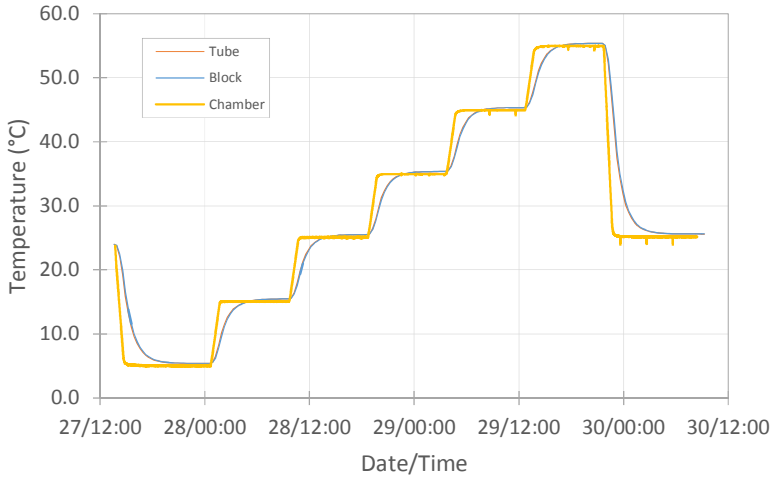

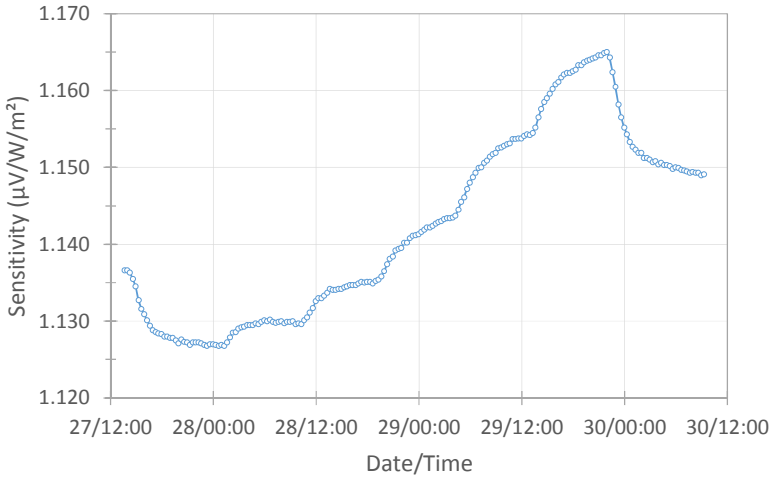

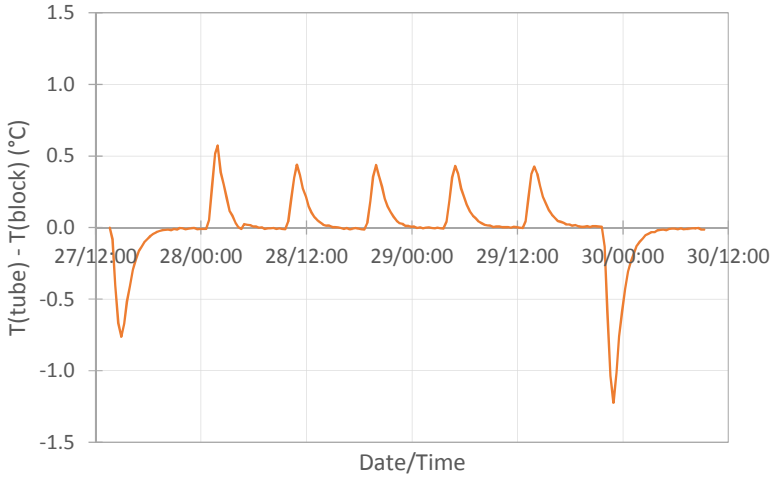

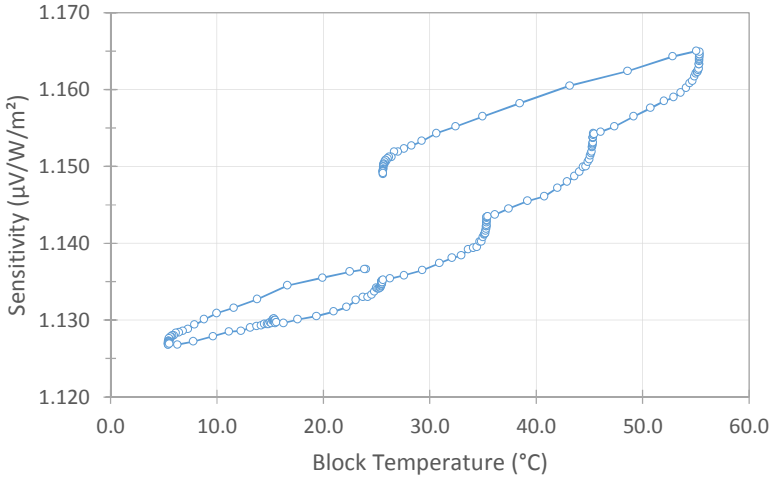

4. Characterization results

➔ Testing on thermopile linearity on electrical power

- Done in the TA *Calibration of Electrical Magnitudes* (PVLab-CIEMAT)
- Check of thermopile output $V_{TE} - V_{T0}$ vs P_E with a Fluke 5520A calibrator as current source, by using Agilent 34970A and Keysight 34420A as meters
- Test at different temperatures inside a climatic chamber

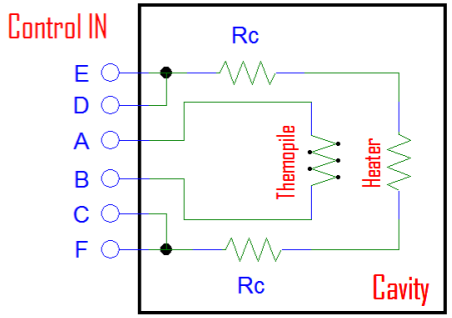

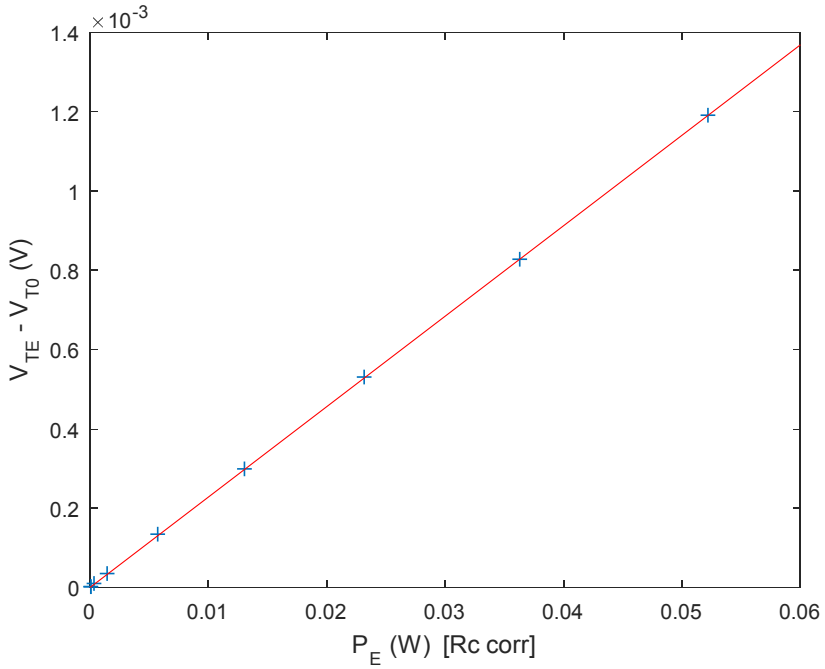

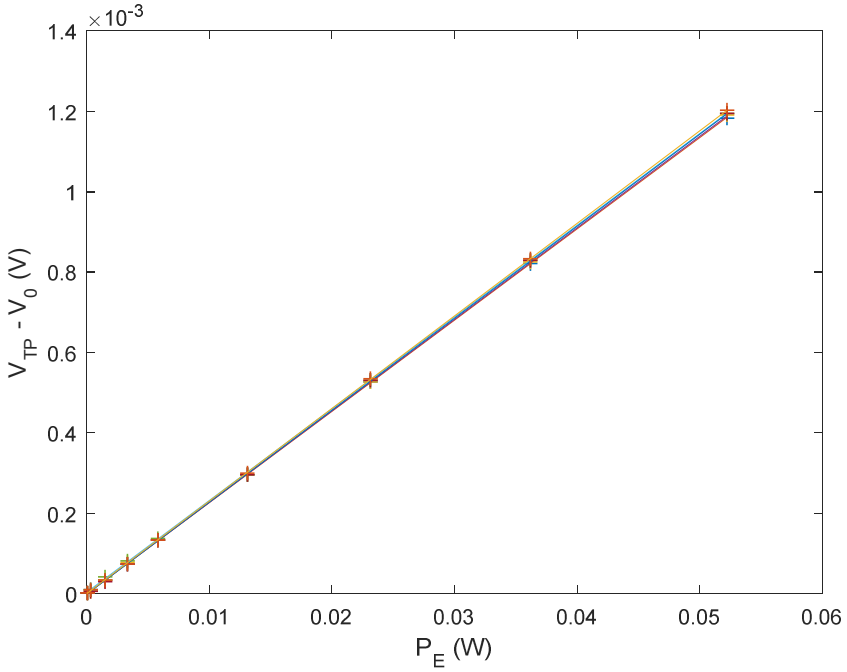

4. Characterization results

➔ Realization of the Electrical Substitution Principle and the non-equivalence factor

- *Equivalence* during AHF operation is realized in terms of (near) *equal powers* instead of *equal temperatures* during open and closed phases.

$$\frac{V_{TS} - V_{T0}}{S} = E = \frac{P_S}{A} \qquad \rightarrow \frac{V_{TS} - V_{T0}}{S} A = P_S \equiv P_E = \frac{V_S^2}{R_H}$$

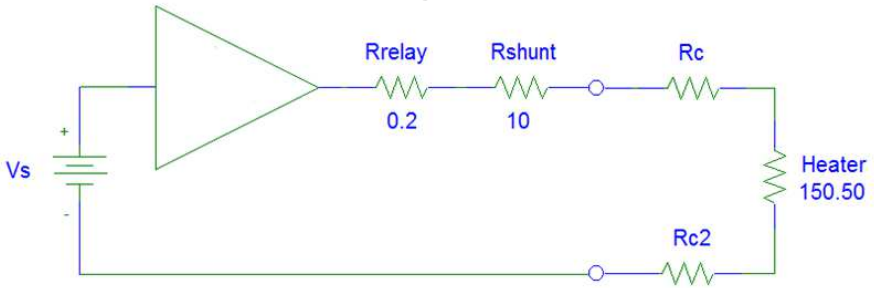

$$\rightarrow V_S = \sqrt{R_H \cdot P_E} + (R_{SH} + R_{rel} + R_C)\sqrt{\frac{P_E}{R_H}}$$

- In practice, this works fine because the thermopile output signal is extremly linear with both radiant and electrical power:

$$1/S = \frac{L}{A \cdot \alpha_C \cdot \gamma}\left(\frac{1}{V_{TE} - V_{T0}}\right) \cdot P_E$$

$$V_{TE} - V_{T0} = k_E \cdot P_E$$

$$\rightarrow k_E = S\frac{L}{A \cdot \alpha_C \cdot \gamma}$$

→ slope

4. Characterization results

➔ **Realization of the Electrical Substitution Principle and the non-equivalence factor**

- Due to this *particular* way to apply the equivalence principle, and the linearity of the thermopile at the normal levels of power (>20mW), it was proposed to use the definition of the non-equivalence factor for directly calculating it

$$L = \frac{k_E}{k_S} \qquad \begin{cases} V_{TS} - V_{T0} = k_S \cdot P_S \\ V_{TE} - V_{T0} = k_E \cdot P_E \end{cases}$$

- Slopes of the stright lines are obtained from a least squares fit
- Both thermopile output signals be measured: 1) with the same instrument (DL) than in normal operation; 2) during the same periods for have equal working conditions
- A reference that determines P_S is needed

→ Data recorded during IPC-XII have been used for this

4. Characterization results

➔ **Realization of the Electrical Substitution Principle and the non-equivalence factor**

- Data recorded during IPC-XII (2015) used for computing slopes
- Uncertainty calculated by Montecarlo method for k_E, k_S

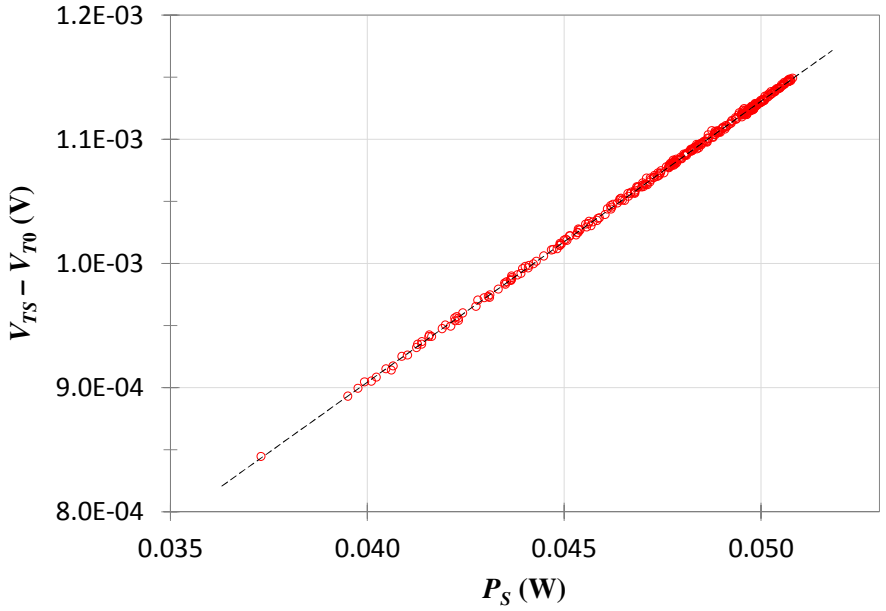

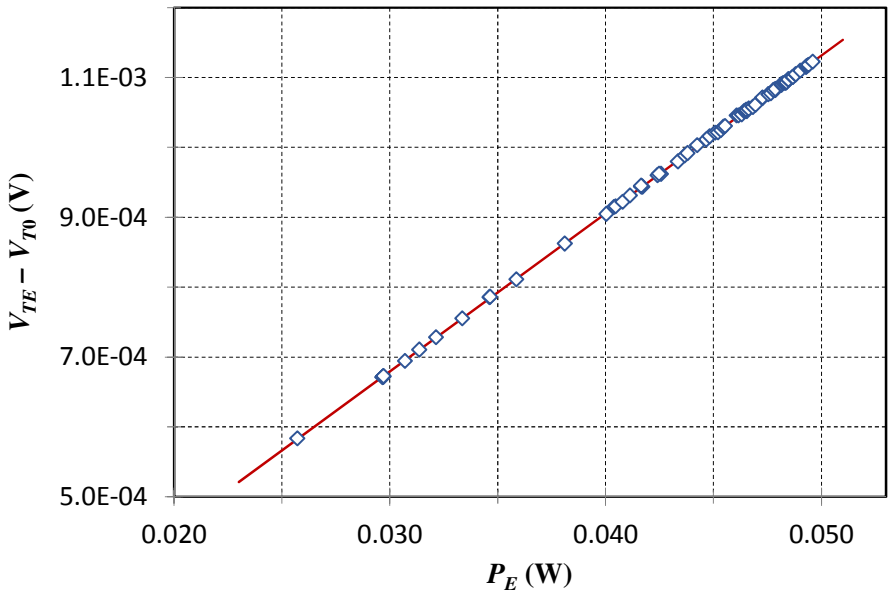

$$L = \frac{k_E}{k_S}$$

k_E = 22.61276 ± 0.01715 mV/W

k_S = 22.61438 ± 0.05026 mV/W

L **= 0.999927 ± 0.004150** (*k*=2)

4. Characterization results

➔ Optical characterization (1)

- Measurement of spectral reflectance (diffuse, hemispherical) of paints and surfaces used in radiometers (for AHF: Chemglaze Z302, Nextel, Invar disk)
- Perkin Elmer Lambda 900 (250-2500nm) and FTIR Frontier (2,5-16µm)

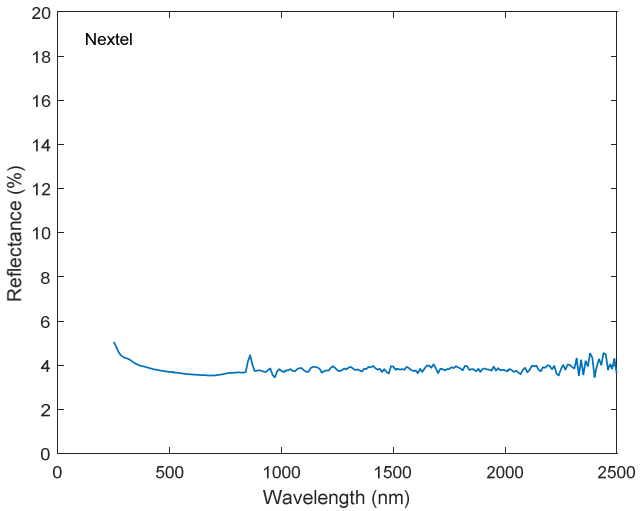

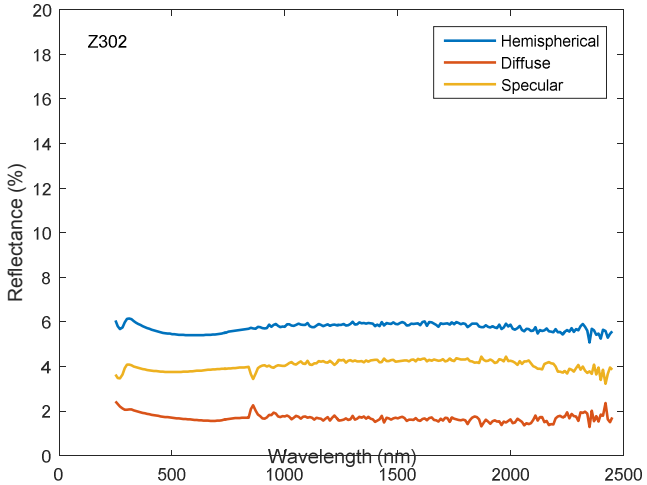

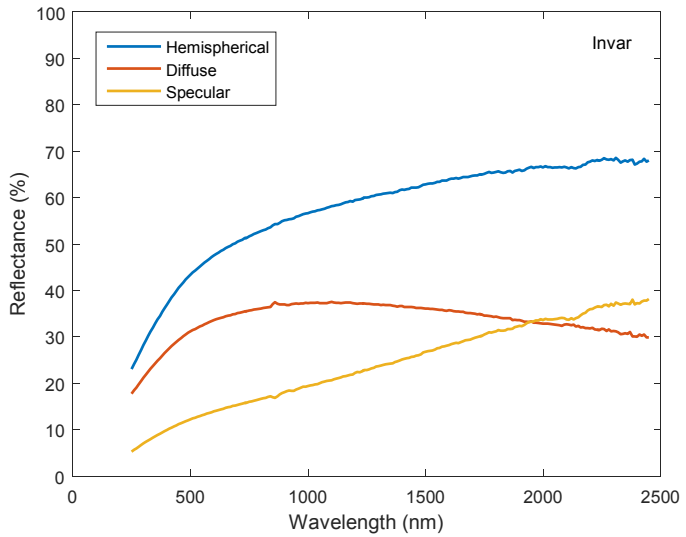

- Calculation of AM1.5D spectral distribution weigthed reflectances

Surface	Reflectance (%)		
	Hemispherical	Specular	Diffuse
Z302	5.6304	3.9366	1.6938
Invar	51.5315	17.2855	34.1270
Nextel	3.7203	0	3.7203

4. Characterization results

➔ Optical characterization (2)

- Numerical calculation of absorptance and distribution of radiation inside the cavity by the method of sums (analysis of blackbody emissivities)
- The model only takes into account paraxial optics.

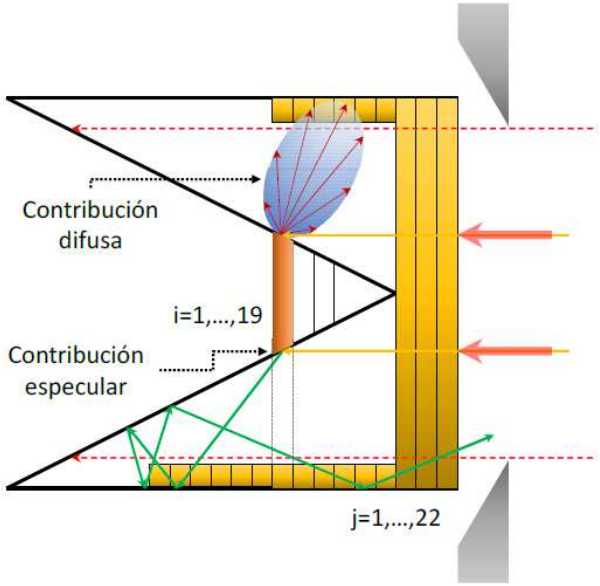

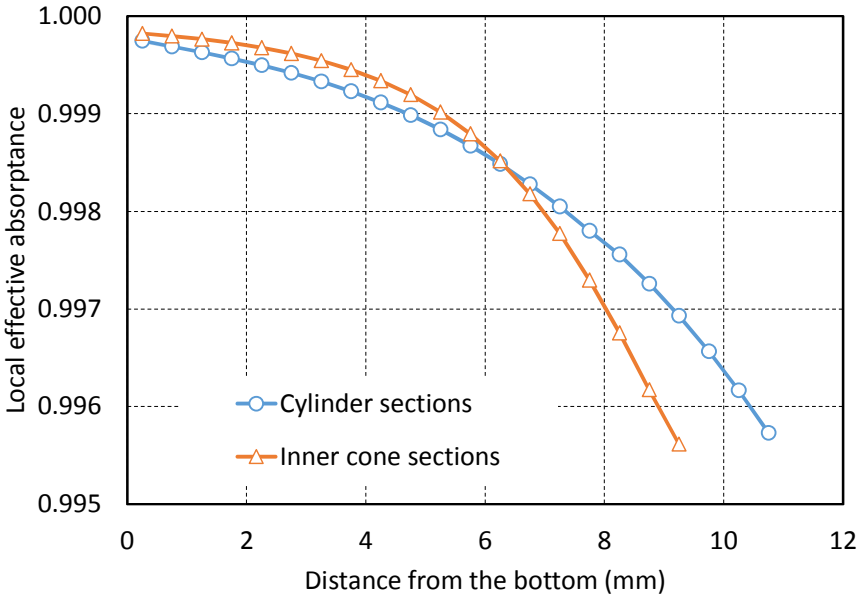

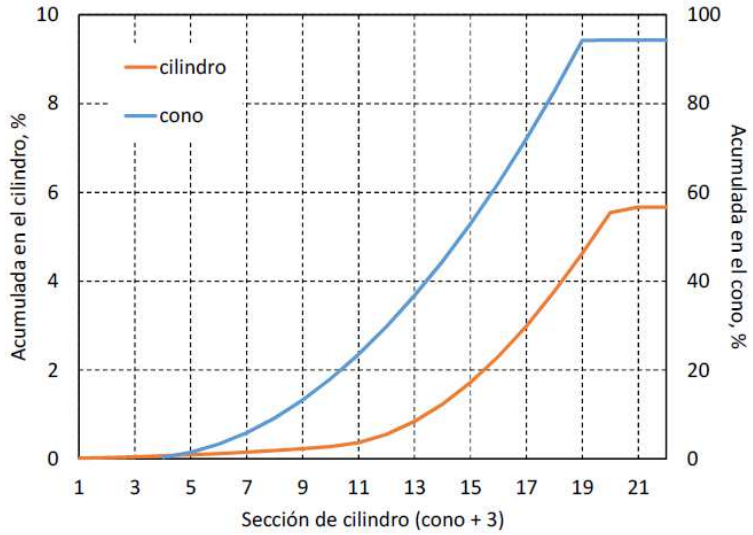

$\alpha_C = 0.99912 \pm 0.00011$

	Percent (%)
Cone	94.3
Cylinder	5.7

4. Characterization results

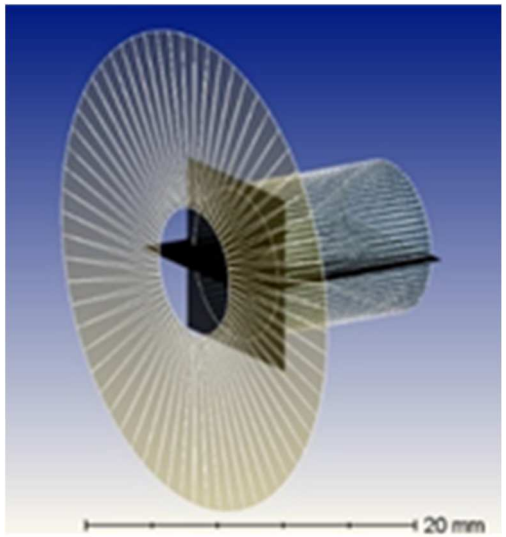

➔ Optical characterization (3)

- Zemax simulation of absortance and reflectance of the cavity

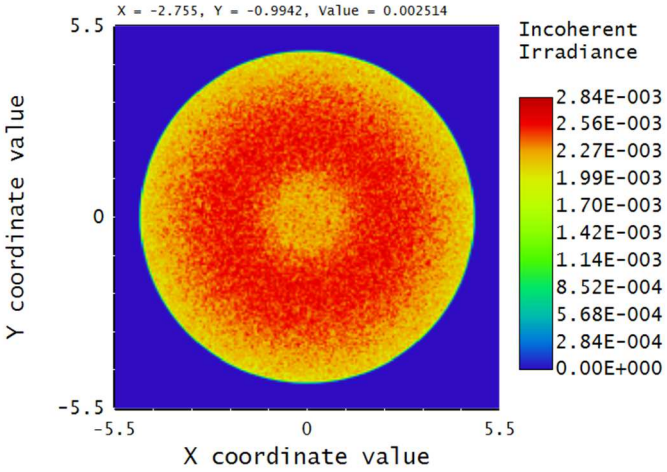

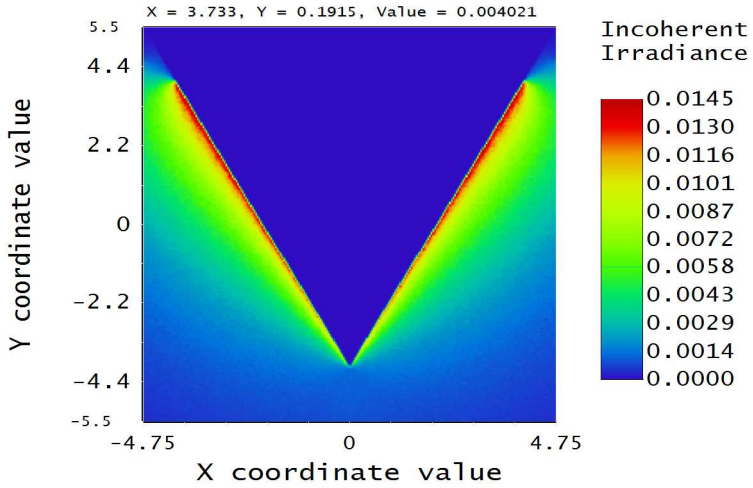

→ Light exiting the cavity is only due to diffuse component of reflectance

Light source	Input Power	Output power	Reflectance	Absorptance
Monochr.	1 W	1.6668E-03 W	1.6668E-03	0.99833
Sun	0.082974	0.00014297 W	0.0017231	0.99828

4. Characterization results

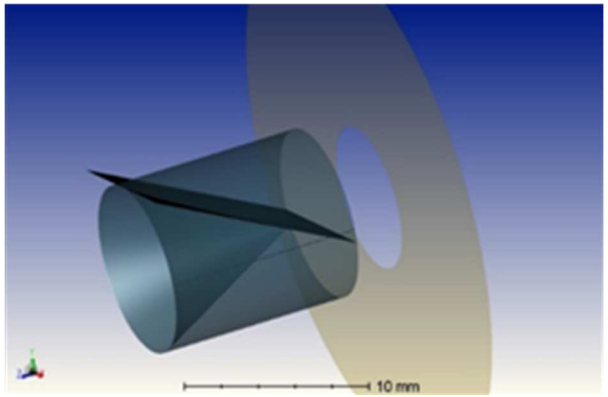

➔ Optical characterization (4)

- Calculation of distribution of irradiance inside the cavity

→ Linear detector in the cylinder

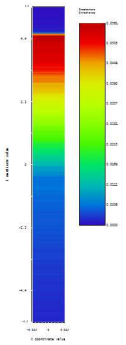

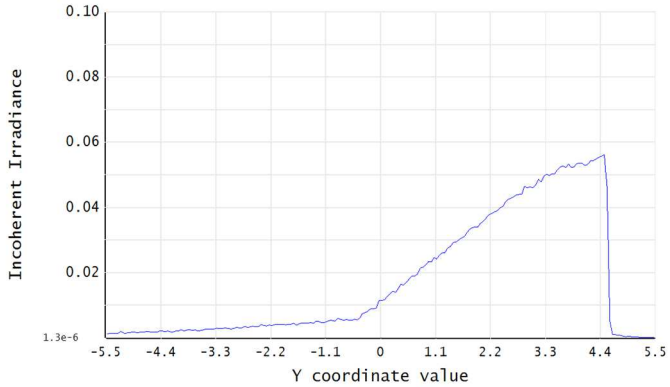

	Surface (mm^2)	detector power (W)	Percent (%)
Cone	157.61	$2.366 \cdot 10^{-3}$	94.42
Cylinder	328.30	$5.608 \cdot 10^{-5}$	5.58

→ Planar detector in the cone

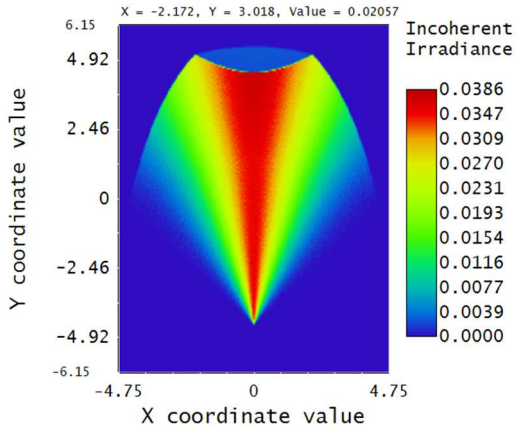

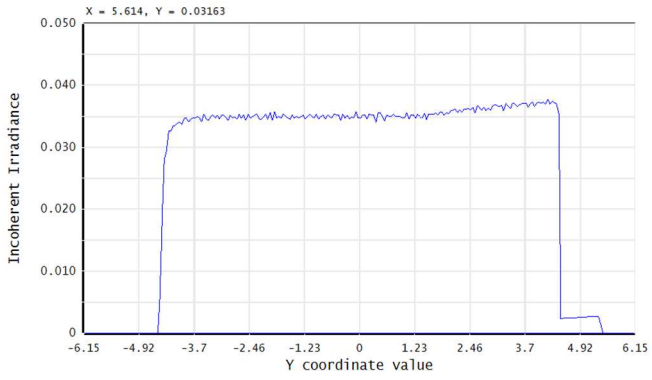

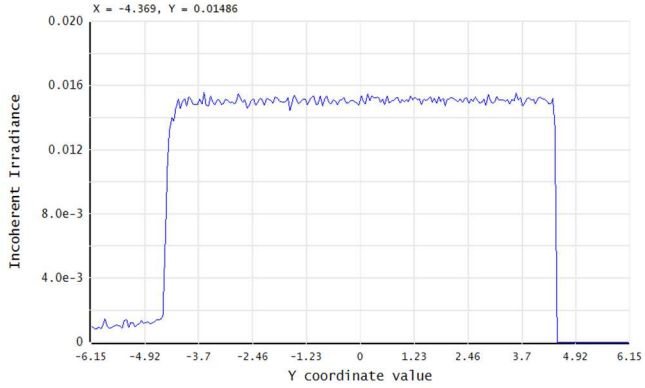

4. Characterization results

➔ Optical characterization (5)

- Zemax simulation of scattering effects due to the collimator tube

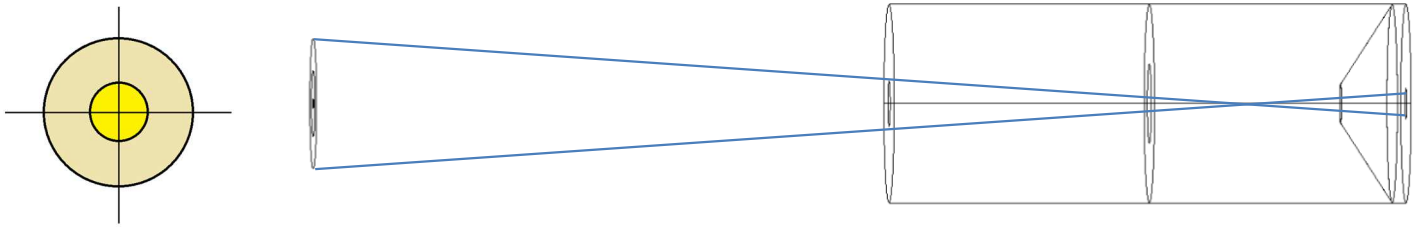

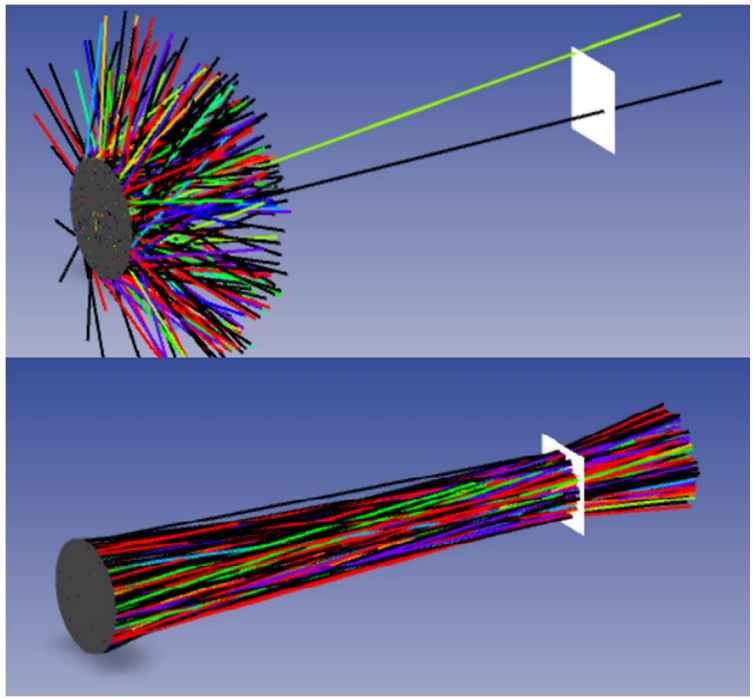

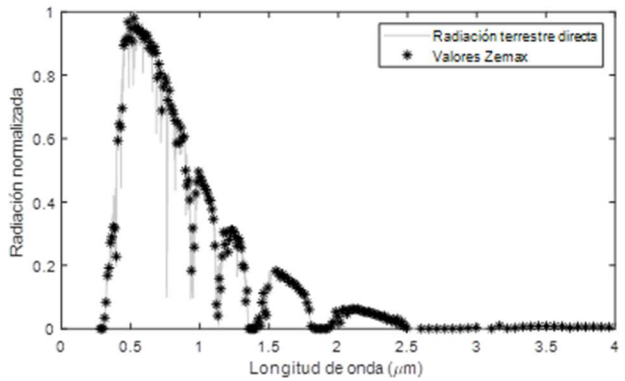

Power w/o collimator	Power w collimator	N	γ (ratio)	SD
3.6890	3.6933	15	1.00117	±0.00098

4. Characterization results

➔ Optical characterization (6)

- Zemax simulation of diffraction effects

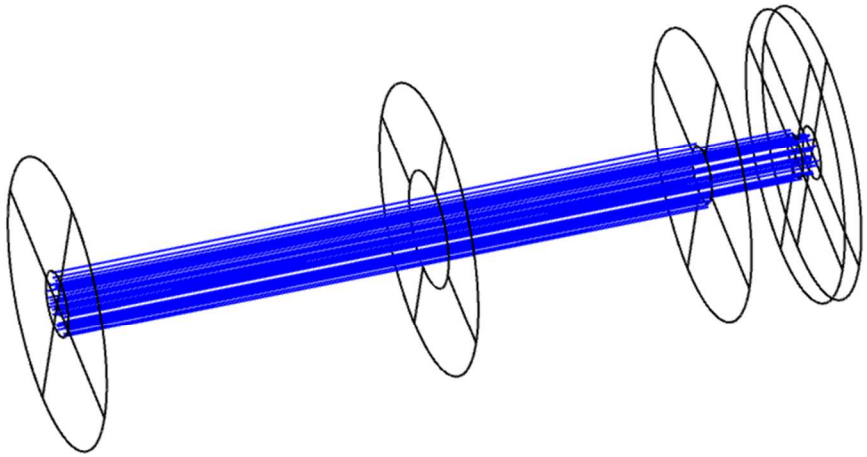

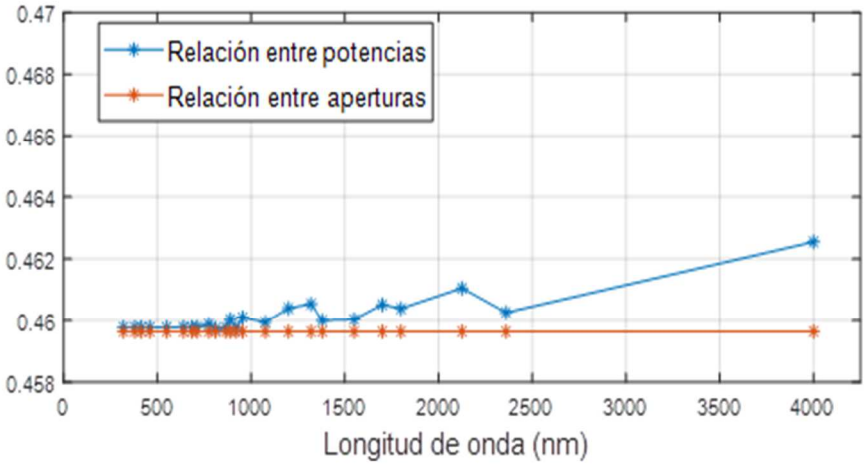

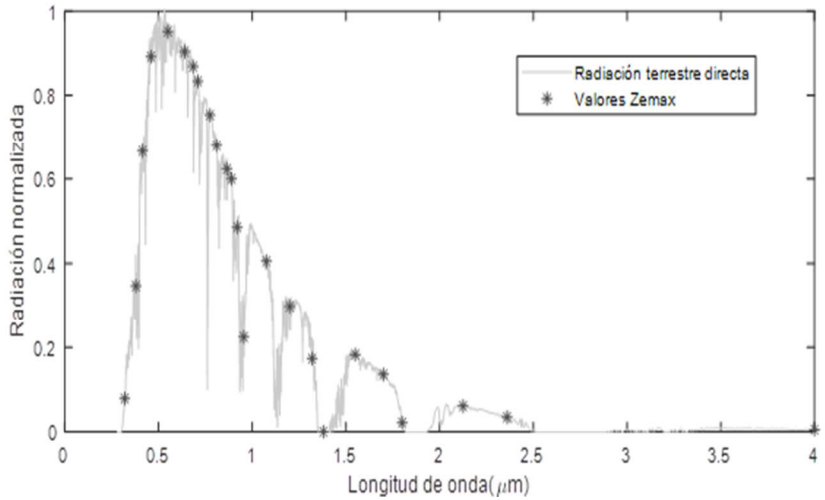

→ Use of a merit function with weigthed spectral distribution for computing diffraction effects

R_{POP} [power]	R_{geo} [area]	Diff. Effect	Correction factor
0.45989	0.45964	1.00054	0.99946

4. Characterization results

➔ Test on difracction/scattering effects

- Setup adapted from a LBIC measurement system of PV solar cells, based on a 632 nm laser and a XY motorized table
- Hamamatsu 1337-1010BQ PD placed in the same position as the cavity, AHF original parts on PLA dummy pieces

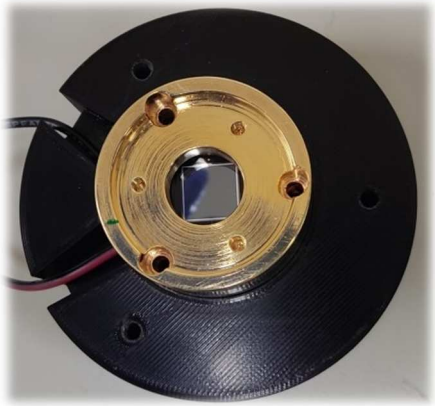

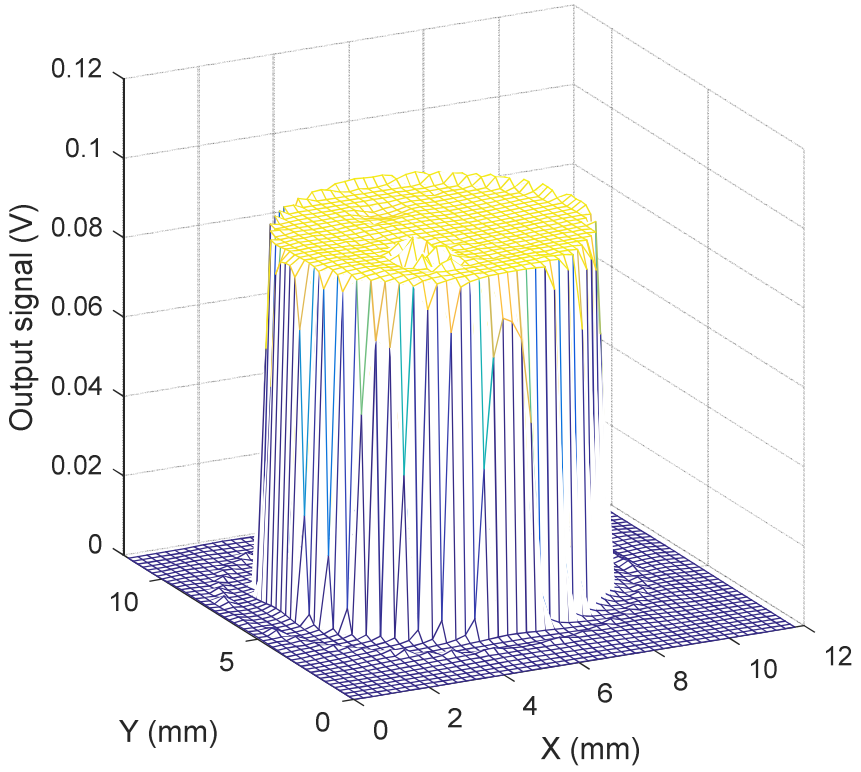

Laser beam ~0.4 mmØ, scanning Δ=0.25 mm, 48×48 grid

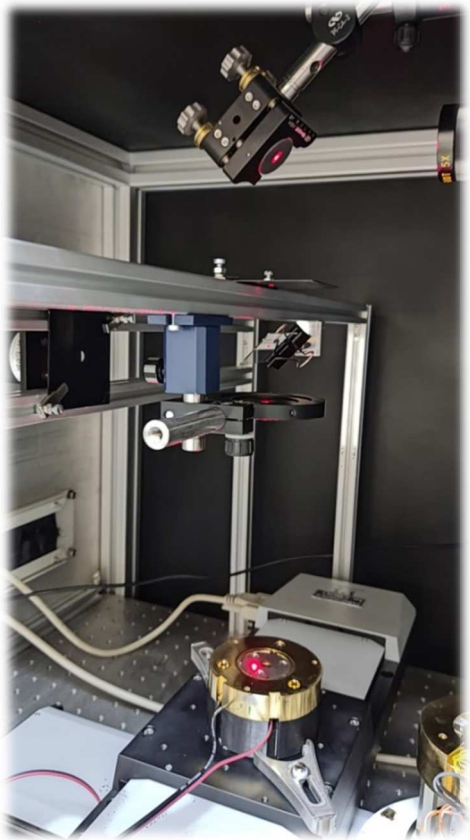

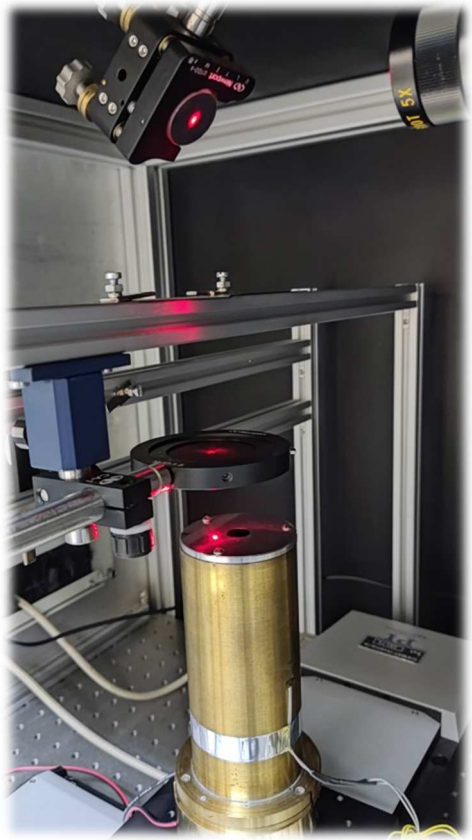

4. Characterization results

➔ Test on difracction/scattering effects

- View in semilog scale reveals two *rings*, corresponding to diaphragms defining FOV of the collimator

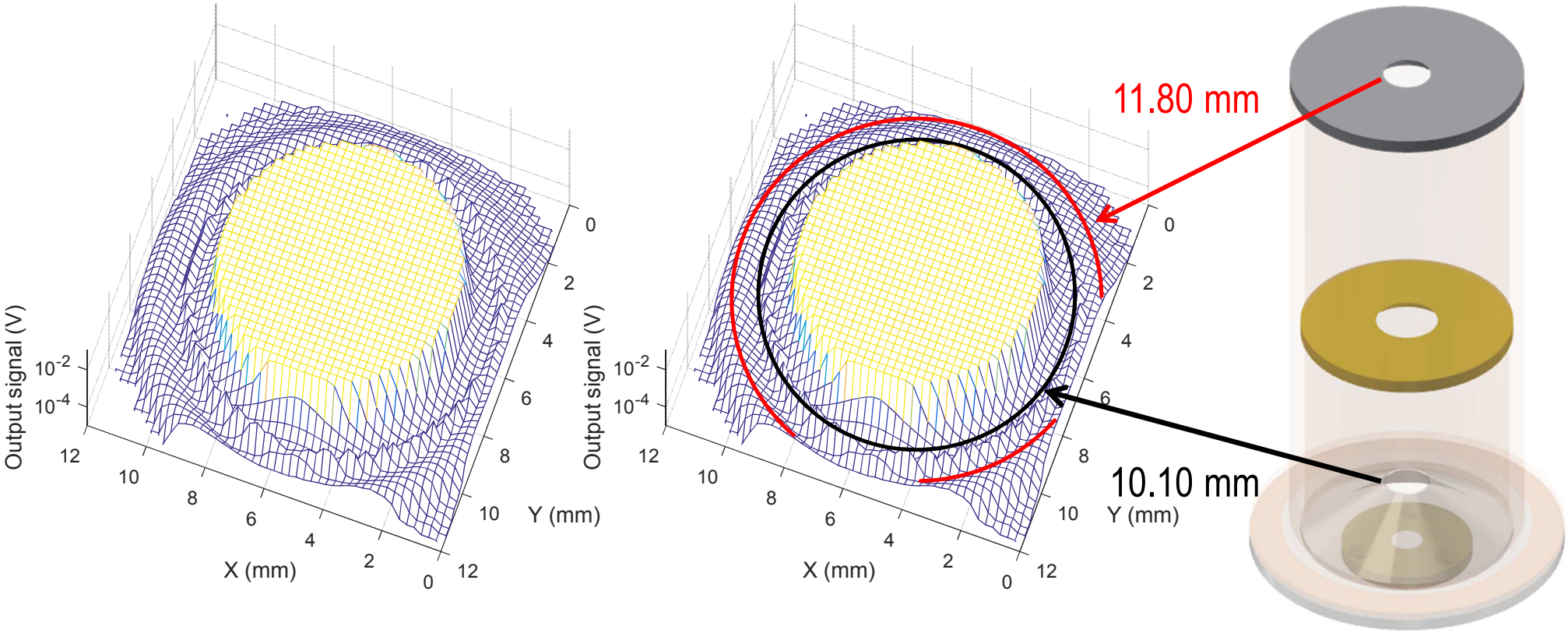

- Posible evidence of diffraction effects
- Improvements in the experimental setup are needed

5. Uncertainty budget

→ Measurement model funtion:

$$E = \frac{L}{A\,\alpha_C\,\gamma}\cdot\left(\frac{V_{TS}-V_{T0}}{V_{TE}-V_{T0}}\right)\cdot\frac{V_I}{R_N}\left(V_H-\frac{V_I}{R_N}R_C\right)$$

→ According to GUM:

$$y = f(x_1,x_2,x_3,\ldots,x_N) \rightarrow u_B^2(y) = \sum_{i=1}^{N}\left[\frac{\partial y}{\partial x_i}\right]^2 u^2(x_i) + 2\sum_{i=1}^{N-1}\sum_{j=i+1}^{N}\frac{\partial y}{\partial x_i}\frac{\partial y}{\partial x_j}u(x_i,x_j)$$

→ In our case, neglecting correlation terms:

$$E = f(L,\alpha_C,A,\gamma,V_{TS},V_{T0},V_{TE},V_I,V_H,R_N,R_C) \rightarrow u_B^2(E) = \sum_{i=1}^{N}\left[\frac{\partial E}{\partial x_i}\right]^2 u^2(x_i)$$

→ For practical reasons, it is better to calculate relative uncertainty:

$$\rightarrow \frac{u_B^2(E)}{E^2} = \sum_{i=1}^{N}\frac{1}{E^2}\left[\frac{\partial E}{\partial x_i}\right]^2 u^2(x_i)$$

5. Uncertainty budget

→ Explicitly:

$$\frac{u_B^2(E)}{E^2} = \frac{1}{E^2}\left[\frac{\partial E}{\partial L}\right]^2 u^2(L) + \frac{1}{E^2}\left[\frac{\partial E}{\partial A}\right]^2 u^2(A) + \frac{1}{E^2}\left[\frac{\partial E}{\partial \gamma}\right]^2 u^2(\gamma) + \frac{1}{E^2}\left[\frac{\partial E}{\partial \alpha_C}\right]^2 u^2(\alpha_C) + \ldots$$
$$+ \frac{1}{E^2}\left[\frac{\partial E}{\partial V_{TE}}\right]^2 u^2(V_{TE}) + \frac{1}{E^2}\left[\frac{\partial E}{\partial V_{TS}}\right]^2 u^2(V_{TS}) + \frac{1}{E^2}\left[\frac{\partial E}{\partial V_{T0}}\right]^2 u^2(V_{T0}) + \ldots$$
$$+ \frac{1}{E^2}\left[\frac{\partial E}{\partial V_H}\right]^2 u^2(V_H) + \frac{1}{E^2}\left[\frac{\partial E}{\partial V_I}\right]^2 u^2(V_I) + \frac{1}{E^2}\left[\frac{\partial E}{\partial R_C}\right]^2 u^2(R_C) + \frac{1}{E^2}\left[\frac{\partial E}{\partial R_N}\right]^2 u^2(R_N)$$

…and after some maths…

$$\frac{u^2(E)}{E^2} = \frac{1}{L^2}u^2(L) + \frac{1}{A^2}u^2(A) + \frac{1}{\alpha_C^2}u^2(\alpha_C) + \frac{1}{\gamma^2}u^2(\gamma)$$
$$+ \frac{u^2(V_{TE})}{(V_{TE}-V_{T0})^2} + \frac{u^2(V_{TS})}{(V_{TS}-V_{T0})^2} + \frac{(V_{TS}-V_{TE})^2}{(V_{TE}-V_{T0})^2(V_{TS}-V_{T0})^2}u^2(V_{T0})$$
$$+ \frac{1}{\left(V_H - \frac{V_I}{R_N}R_C\right)^2}\left[u^2(V_H) + \left(\frac{V_I}{R_N}\right)^2 u^2(R_C) + \left(V_H - 2\frac{V_I}{R_N}R_C\right)^2 \cdot \left(\frac{u^2(V_I)}{V_I^2} + \frac{u^2(R_N)}{R_N^2}\right)\right]$$

5. Uncertainty budget

Term	Estimate Test value	Uncertainty (k=1)	Sensitivity coeff. S / E	Contribution ($\times 10^{-6}$)	Relative contribution
L	0.999 927	0.002 075	1.0001	2075.4	56.62 %
A	50.183 mm^2	0.007 5 mm^2	0.019927 mm^{-2}	149.5	0.29 %
α_C	0.999 12	0.000 06	1.0009	61.2	0.05 %
γ	1.001	0.000 5	0.9990	500.0	3.29 %
V_{TE}	0.956 152 mV	0.002 344 mV	1.0452 mV^{-1}	1235.6	20.07 %
V_{TS}	0.966 129 mV	0.002 344 mV	1.0344 mV^{-1}	1223.3	19.67 %
V_{T0}	-0.624 680 µV	0.002 338 mV	0.010786 mV^{-1}	12.6	0.00 %
V_H	2.508 384 V	0.000 081 V	0.39884 V^{-1}	16.8	0.01 %
V_I	0.166 645 V	0.000 0081 V	5.9981 V^{-1}	25.7	0.01 %
R_C	50.990 7 mΩ	0.003 4 mΩ	6.6464×10^{-3} mΩ^{-1}	22.3	0.01 %
R_N	9.998 69 Ω	0.000 055 Ω	0.099956 Ω^{-1}	5.5	0.00 %
	TOTAL u		**(k=1)**	**2758**	100.0 %

6. Tracebility to WRR/SI

➔ **Clarifying the method proposed for determining non-equivalence factor *L***

- Seems not to be independent of the radiant source (*should it…?*)
- Seems not to be independent of the reference instruments used for defining the radiant power (W) (*should it…?*)
- Seems to be only valid for comparisons against WRR
- It is the largest contribution to the net uncertainty

→ Pending of comparison against trap detectors/cryogenic radiometers of the SI lab scale in IO-CSIC (DI of the Spanish NMI) to confirm

→ Looking for alternative methods of determination of L

→ Experiment in vacuum chamber to evaluate the effect of air convection

6. Tracebility to WRR/SI

➔ **Additional details we want to improve (not all required to finish)**

- Evaluation of uncertainty of figures (scattering, diffraction) obtained from Zemax
- Experiment to measure/detect diffraction with the laser beam
- Understanding on the thermal effects on sensitivity
- Add a new micro-voltmeter for readings of thermopile signal, to get lower uncertainty
- Apply all these corrections to our measurements to analyze how much our IPC factor would change.
- Publish…

➔ **Next steps**

- Extend the methodology to other cavity radiometers. PMO6 is on the way… maybe PMO8…
- To design and to build our own cavity…? Let's see… In the future…

Conclusions

- → General process of characterization of radiomenters has been explained, and how it has been adapted to the case of AHF
- → Experiments and simulations already carried out have been detailed
- → Uncertainty budget has been calculated on the basis of the model function. Current figure is about ≈2800 ppm, pending of reviewing some contributions
- → Several troubles and future work on AHF characterization has been also pointed out.

Calls

- → to manufacturers/designers: make your cavities modular, easy to take sensors and components apart for calibration and testing; have spare parts, materials, paints, sensors, etc, available for further research
- → to other laboratories/researchers: try to characterize, to calibrate and to know your instruments

On the characterization of an AHF cavity radiometer and its traceability to WRR/SI

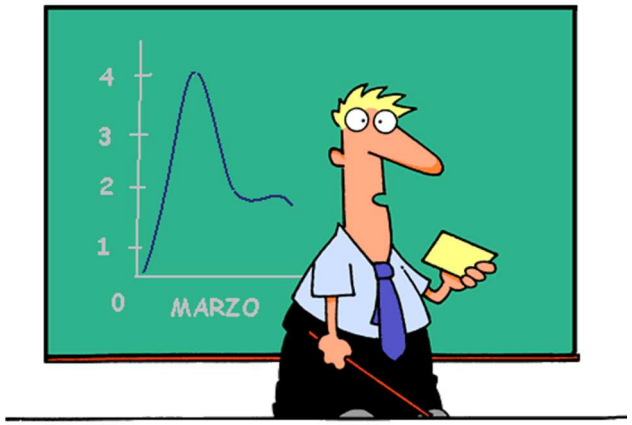

→ **Thank you for your attention**

José Lorenzo Balenzategui
CIEMAT (Spain)
jl.balenzategui@ciemat.es

→ **Thanks a lot to all my colleagues contributing on this…**

→ **It's your turn… shoot!**